A Study of the Surface Region of the Mo−V−Te−O Catalysts for Propane Oxidation to Acrylic Acid

Vadim V. Guliants* and Rishabh Bhandari

Department of Chemical and Materials Engineering, University of Cincinnati, Cincinnati, Ohio 45221-0012

Hidde H. Brongersma and Arie Knoester

Calipso B.V. and Department of Applied Physics, Eindhoven University of Technology, P.O. Box 513, 5600 MB Eindhoven, The Netherlands

Anne M. Gaffney and Scott Han

Rohm and Haas Co., 727 Norristown Road, Spring House, Pennsylvania 19477-0904

Received: December 25, 2004; In Final Form: March 31, 2005

The bulk mixed Mo−V−Te oxides possess high activity and selectivity in propane oxidation to acrylic acid and represent well-defined model catalysts for studies of the surface molecular structure−activity/selectivity relationships in this selective oxidation reaction. The elemental compositions, metal oxidation states, and catalytic functions of V, Mo, and Te in the surface region of the model Mo−V−Te−O system were examined employing low energy ion scattering (LEIS) and X-ray photoelectron spectroscopy (XPS). This study indicated that the surfaces of these catalysts are terminated with a monolayer, which possesses a different elemental composition from that of the bulk. The rates of propane consumption and formation of propylene and acrylic acid depended on the topmost surface V concentration, whereas no dependence of these reaction rates on either the surface Mo or Te concentrations was observed. These findings suggested that the bulk Mo−V−Te−O structure may function as a support for the unique active and selective surface monolayer in propane oxidation to acrylic acid. The results of this study have important practical consequences for the development of improved selective oxidation catalysts by introducing surface metal oxide components to form new surface active V−O−M sites for propane oxidation to acrylic acid.

1. Introduction

The current abundance and low cost of light alkanes has generated much recent interest in the oxidative catalytic conversion of alkanes to olefins, oxygenates (i.e., acrolein and acrylic acid), and nitriles in the petroleum and petrochemical industries.[1−17] This represents the shift in technology from petroleum-based alkene feedstocks to abundant, lower cost, and environmentally friendly natural gas-based alkanes. The propane oxidation to oxygenates and ammoxidation to acrylonitrile are currently of particular interest in view of the importance of these chemical intermediates for the manufacture of acrylate esters used in apparel and home furnishings, copolymers with excellent gas barrier properties, paints, adhesives, and biocides.[18]

The recently discovered multicomponent Mo−V−M−O (M = combinations of Nb, Te, Sb, etc.) catalytic system was reported to be active and selective for one-step propane oxidation to oxygenates and ammoxidation to acrylonitrile.[4−11,19−24] These mixed metal oxides are prepared in aqueous medium by reacting metal oxide sources, e.g. ammonium heptamolybdate, vanadyl sulfate, tellurium dioxide, and ammonium niobium oxalate, at 353−433 K, and calcining in an inert N_2 environment to prevent the phase separation of metal oxide components. The catalysts obtained consist of layered Mo−V−Te−Nb−O phases with a 4 Å *d*-spacing that are commonly observed in multicomponent solid solutions of V, Nb, and other metal ions in Mo^{5+}/Mo^{6+} suboxides.[12−17,25−32] The Mo−V−Te−Nb−O catalysts are obtained as a mixture of two crystalline phases, so-called "M1" and "M2", which were initially proposed as responsible for the propane activation to propylene and its subsequent ammoxidation to acrylonitrile, respectively.[33] The elemental compositions and structures of the catalytic M1 and M2 phases have been investigated recently.[12−16,34−37] The M1 and M2 phases were shown to have respectively orthorhombic and pseudohexagonal crystal structures[37] with $(Te_2O)M_{20}O_{56}$ and $(TeO)M_2O_9$ (M = Mo, V, Nb) compositions.[13,14,16,34] The studies of propane (amm)oxidation indicated that the orthorhombic phase is the most active and selective for both of these transformations, although a synergism due to cooperation between these phases was observed at high propane conversion.[14,16,38] Although the pseudohexagonal M2 phase was unable to activate propane, it was efficient in both propylene ammoxidation to acrylonitrile[14,15] and its oxidation to acrylic acid[16,28] and also showed a higher selectivity to acrylonitrile than the M1 phase.[38]

The M1 and M2 phases possessing well-defined rodlike crystal morphology were also obtained hydrothermally in the Nb-free system ($Mo_{0.6}V_{0.3}Te_{0.1}$) that showed moderate selectivity in transforming ethane and propane to ethylene and acrylic acid, respectively.[12,17,27,35] Therefore, the model Mo−V−Te−O system appeared to be particularly promising for studies of the surface molecular structure−activity/selectivity relationships in selective transformation of propane to oxygenates and acrylo-

* Address correspondence to this author. Phone: +1-513-556-0203. Fax: +1-513-556-3473. E-mail: vadim.guliants@uc.edu.

10.1021/jp044120v CCC: $30.25
Published on Web 04/30/2005

nitrile due to its compositional simplicity and well-defined crystal morphology.

In previous studies,[30,39−41] we investigated the synthesis phase diagram of this model catalytic system and observed the formation of the M1 and M2 phases under a wide range of hydrothermal synthesis conditions. We further studied the crystal structures as well as the bulk and local chemical compositions of the M1 and M2 phases present in the Mo−V−Te−O system by high-resolution transmission electron microscopy (HRTEM), EDS, and ICP elemental analysis.[39] The three synthesis compositions reported previously ($Mo_{0.6}V_{0.3}Te_{0.1}$, $Mo_{0.5}V_{0.4}Te_{0.1}$, and $Mo_{0.3}V_{0.6}Te_{0.1}$) contained essentially pure M1 phase and only trace amounts of the M2 phase.[30] Similar to the optimized Mo−V−Te−Nb−O system,[4,19−24] the model Mo−V−Te−O catalysts displayed relatively high yields of acrylic acid, which correlated with the exposure of the surface basal *ab* planes in these catalysts.

In this report, we extended the study of the model Mo−V−Te−O system to examine the elemental compositions, metal oxidation states, and catalytic functions of V, Mo, and Te in the surface region of the three model catalysts reported by us previously[30] employing low energy ion scattering (LEIS) and X-ray photoelectron spectroscopy (XPS). This study indicated that the surfaces of these catalysts are terminated with a monolayer, which possesses a different elemental composition from that of the bulk. Therefore, these findings suggested that the bulk Mo−V−Te−O structure functions as a very special support for the unique active and selective surface monolayer in propane transformation to oxygenates and acrylonitrile.

2. Experimental Section

2.1. Catalyst Preparation. The mixed Mo−V−Te−O catalysts were prepared hydrothermally with ammonium paramolybdate (Alfa Aesar, 81−83% as MoO_3), vanadyl(IV) sulfate (Alfa Aesar, 99.9%), and TeO_2 (Alfa Aesar, 99.99%) as the metal oxide sources. In a typical synthesis, exemplified here for the $Mo_{0.6}V_{0.3}Te_{0.1}$ composition, ammonium paramolybdate (6.80 g, 38.7 mmol of Mo^{6+}) was dissolved in 100 mL of deionized water with stirring at room temperature. TeO_2 (0.96 g, 6.0 mmol of Te^{4+}) was added to the resulting solution leading to a white suspension and the mixture was stirred for 0.5 h. Vanadyl(IV) sulfate (4.68 g, 19.2 mmol of V^{4+}) was dissolved in 60 mL of deionized water at room temperature and added dropwise to the Mo−Te suspension. The mixture became viscous brown upon V^{4+} addition, then a dark pink homogeneous gel. The resultant gel was placed in a Teflon-lined stainless steel autoclave and heated for 72 h at 175 °C. The black solid was filtered, washed with deionized water, and dried for 12 h at 80 °C. The mixed metal oxide product was calcined at 600 °C for 2 h under flowing N_2 (40−60 cm^3/min) in a tubular furnace. The temperature was ramped to 600 °C at 5 °C/min^{-1}.

2.2. Kinetic Studies. The kinetic studies of propane oxidation were conducted at 350−450 °C, using a 48 mL/min feed of 6.3 vol % of propane, 9.4 vol % of oxygen, 47.3 vol % of water vapor, and balance of He and 1.0 g of catalyst packed in a $^3/_8$ in. quartz tubular microreactor in a programmable oven. An HP 5890II gas chromatograph equipped with an FID and TCD was employed for the reaction product analysis. The carbon balances agreed within 5 mol %.

2.3. Physicochemical Characterization. The model Mo−V−Te−O catalysts were characterized by powder X-ray diffraction (XRD) employing a Siemens D500 diffractometer (Cu Kα radiation). The ICP elemental composition was determined with a Leeman Labs ICP/Echelle spectrometer, Model PS1000 ICP, equipped with a Hildebrand Grid nebulizer and Mo, V, and Te elemental standards (Alfa Aesar). The BET surface areas were determined from the N_2 adsorption isotherms ($0.05 < P/P_o < 0.3$) at −196 °C employing a Micromeritics TriStar 3000 porosimeter. The EDS analysis of the local elemental composition was conducted at the Argonne National Laboratory with a Philips CM30 transmission electron microscope operated at 200 kV and equipped with an EDAX-NX2 (spatial resolution ∼1 nm) for the local composition analysis. MoO_3, V_2O_5, and TeO_2 were used as the EDS elemental standards to determine the respective Cliff−Lorimer sensitivity *k*-factors.

The XPS measurements of pressed model catalysts were carried out on a Perkin-Elmer Model 5300 XPS spectrometer with Mg Kα 1253.6 eV radiation at 300 W. Survey spectra and high-resolution spectra were obtained with use of pass energies of 89.45 and 35.75 eV, respectively. The Perkin-Elmer software was used for data acquisition and processing. The binding energy of C 1s was set to 284.5 eV and used as a reference to correct the binding energies (BE) of other elements for sample charging. The XPS spectra were recorded at takeoff angles of 15°, 45°, and 75°. The accuracy of the reported BE energies was ±0.1 eV and the quantitative analysis of the XPS data had an estimated error of ca. 10%.

The LEIS analysis of model catalysts after kinetic studies was performed employing a Calipso LEIS system equipped with a highly sensitive double toroïdal analyzer (3000× that of other LEIS analyzers). The Calipso LEIS system is a unique surface characterization tool with a sampling depth of one atomic layer.[42] In LEIS, the sample is bombarded with low-energy noble gas ions that are subsequently scattered by surface atoms. The backscattered ions are then energy analyzed in an electrostatic analyzer and their energies are related to the scattering elements by the laws of conservation of energy and momentum. The noble gas ions have high electron affinities and hence high neutralization probability on interaction with the surface. This restricts the information depth to one atomic layer as the ions penetrating the first layer have longer interaction time with the sample and thus will be effectively neutralized. Hence the signals coming from the multiple reflections can generally be neglected. Thus, the obtained spectra can be interpreted essentially as the mass spectra of surface atoms. During the studies, the damage inflicted upon the surface is negligible due to the low ion doses. Three model catalysts with synthesis compositions corresponding to $Mo_{0.6}V_{0.3}Te_{0.1}$, $Mo_{0.5}V_{0.4}Te_{0.1}$, and $Mo_{0.3}V_{0.6}Te_{0.1}$ were analyzed by LEIS. The following surfaces were analyzed: the original surfaces after kinetic studies, the surfaces after treatment with atomic oxygen for 5 min to remove carbonaceous deposits and environmental contaminants, the surfaces after sputtering of ca. 1 atomic layer (ML) with Ne^+ ions, the surface of the $Mo_{0.3}V_{0.6}Te_{0.1}$ catalyst after sputtering of ca. 2 ML with Ne^+ ions, and the surface of $Mo_{0.5}V_{0.4}Te_{0.1}$ catalyst after 10 min at 400 °C.

The samples were prepared for LEIS by pressing powdered catalyst into thin tablets at 300 MPa. It has been shown before[43] that at this pressure a reliable quantitative analysis is possible, while the structure and atomic composition of the outer surface are not affected. The treatment with atomic oxygen for 5 min was employed to remove environmental contaminants and/or carbonaceous product species from the original surface of the catalysts after kinetic studies. Oxidized Te surface was obtained by treating elemental Te (Johnson Matthey Chemical Ltd) with atomic oxygen for 20 min. This was used as a Te oxide standard in the LEIS measurements. This oxidized Te oxide surface consisting of Te atoms partially shielded by O atoms reflected

TABLE 1: Propane Oxidation to Acrylic Acid (AA) at 380 °C over Model Mo−V−Te Oxide Catalysts[a]

catalyst	S_{BET}, m^2/g	$C_{C_3H_8}$, mol %	$S_{C_3H_6}$, mol %	S_{AA}, mol %	S_{CO}, mol %	S_{CO_2}, mol %
$Mo_{0.6}V_{0.3}Te_{0.1}$	7.6	28	21	49	18	12
$Mo_{0.5}V_{0.4}Te_{0.1}$	6.4	34	7	67	16	11
$Mo_{0.3}V_{0.6}Te_{0.1}$	1.9	20	13	64	6	17

[a] Experimental conditions: feed of 6.3 vol % of C_3H_8, 9.4 vol % of O_2, 47.3 vol % of H_2O, and the balance He at 48 mL/min; 1 g of catalyst. $C_{C_3H_8}$ = 100[total moles of C_3H_8 converted]/[moles of C_3H_8 in feed]. S_i = 100[moles of C_3H_8 converted to product i]/[total moles of C_3H_8 converted]. Yield, $Y_i = C_{C_3H_8}(S_i/100)$.

the "visibility" of the Te atoms in the mixed metal oxide catalysts of the present study.

The analysis was performed with both $^4He^+$ and $^{20}Ne^+$ ions at 3 keV. $^4He^+$ scattering was used to detect surface O, V, and the combined presence of Mo and Te atoms. Since the Mo and Te signals were not resolved in the $^4He^+$ spectra, $^{20}Ne^+$ ions were used to separate contributions of these two elements. However, the O and V signals are not detected in the Ne^+ spectra. Moreover, the Mo and Te sensitivity factors in the $^4He^+$ spectra differ from those in the $^{20}Ne^+$ spectra. Therefore, the signal intensity ratio for one of these two elements from the $^4He^+$ and the $^{20}Ne^+$ spectra was required in order to separate the Te and Mo contributions in their combined LEIS peak in the$^4He^+$ spectra. Therefore, the oxidized Te reference powder was measured with both $^4He^+$ and $^{20}Ne^+$ ions to determine the Ne/He signal ratio for Te. Finally, the Te and Mo contributions to the combined Mo/Te peaks in the $^4He^+$ spectra were determined by using this ratio (i.e. 7.68).

The sensitivity factors for V, Mo, and Te were found from the signal yields obtained in the $^4He^+$ spectra. The Te sensitivity factor (SF_{Te}) was directly determined from the $^4He^+$ spectrum of the Te oxide reference sample. The best estimates of V and Mo sensitivity factors (SF_V and SF_{Mo}) were obtained by solving a system of two equations with two unknowns (SF_V and SF_{Mo}), using the LEIS signal yields (S_V, S_{Mo}, and S_{Te}) of two different catalysts after atomic oxygen treatment:

$$S_V/SF_v + S_{Mo}/SF_{Mo} + S_{Te}/SF_{Te} = 1$$

The equations obtained from the LEIS data for different sets of catalyst samples yielded slightly different V and Mo sensitivity factors. The finally chosen "best estimates" of SF_V and SF_{Mo} yielded combined (Mo + V + Te) surface concentrations for the mixed Mo−V−Te−O catalysts that were close to 100% for all catalysts.

3. Results

The catalytic properties of the three model catalysts ($Mo_{0.6}V_{0.3}Te_{0.1}$, $Mo_{0.5}V_{0.4}Te_{0.1}$, and $Mo_{0.3}V_{0.6}Te_{0.1}$) in propane oxidation to acrylic acid and their bulk characteristics were reported previously[30] and are summarized in Tables 1 and 2. The bulk characterization revealed that these model catalysts contained essentially pure M1 phase with trace amounts of the M2 phase.[30] The content of the trace M2 impurity in the $Mo_{0.3}V_{0.6}Te_{0.1}$ catalyst was slightly higher than that in the other two catalysts.

The X-ray photoelectron spectroscopy (XPS) was employed to gain insights into elemental composition and oxidation states of metal ions in the surface region of these bulk mixed metal oxide catalysts (Tables 2 and 3). The XPS spectra were collected at takeoff angles of 15°, 45°, and 75° to determine surface region compositions for different escape depths. These XPS spectra obtained revealed a negligible variation in the surface-region concentrations for Mo, V, and Te. The XPS spectra collected at a 45° takeoff angle for the three model catalysts after kinetic studies are shown in Figure 1. The average XPS elemental compositions for the three takeoff angles are reported in Table 2. The surface-region XPS compositions of the Mo−V−Te−O catalysts were similar to their bulk (ICP) compositions.

The oxidation states of metal ions in these mixed metal oxide catalysts were also determined by XPS (Table 3). The C 1s signal at 284.5 eV was used as a reference peak to correct for a shift in the binding energies (BE) due to sample charging. The binding energies of Te and Mo determined with use of the TeO_2 and MoO_3 references were similar to the published values.[44] The binding energy of the V_2O_5 reference was determined to be 517.0 eV, which is slightly different from the reported value of 517.6 eV.[44] This shift is probably due to the reduction of the V_2O_5 reference. The Te peaks in the model Mo−V−Te−O catalysts were found in the 576.1−576.4 eV range, indicating that Te was likely to be in both 6+ and 4+ oxidation states. The Mo 3d core level peaks were found in the 232.5−232.8 eV range, corresponding to a mixture of 6+ and 5+ oxidation states. The V binding energies in these catalysts (516.3−517.1 eV) also suggested a mixture of 5+ and 4+ oxidation states. The binding energies did not change appreciably before and after kinetic studies.

TABLE 2: Surface-Region Compositions (XPS) of Mo−V−Te−O Catalysts Before and After Kinetic Studies (KS)

synthesis composition	$Mo_{0.60}V_{0.30}Te_{0.10}$	$Mo_{0.50}V_{0.40}Te_{0.10}$	$Mo_{0.30}V_{0.60}Te_{0.10}$
ICP composition (after KS)	$Mo_{0.60}V_{0.27}Te_{0.09}$	$Mo_{0.50}V_{0.30}Te_{0.05}$	$Mo_{0.30}V_{0.24}Te_{0.06}$
M1 (TEM/EDS)	$Mo_{0.60}V_{0.32}Te_{0.07}$	$Mo_{0.50}V_{0.30}Te_{0.22}$	$Mo_{0.30}V_{0.15}Te_{0.05}$
M2 (TEM/EDS)	$Mo_{0.60}V_{0.76}Te_{0.08}$	$Mo_{0.50}V_{0.74}Te_{0.16}$	$Mo_{0.30}V_{0.31}Te_{0.02}$
XPS composition (before KS)	$Mo_{0.60}V_{0.19}Te_{0.05}$	$Mo_{0.50}V_{0.39}Te_{0.12}$	$Mo_{0.30}V_{0.27}Te_{0.06}$
XPS composition (after KS)	$Mo_{0.60}V_{0.25}Te_{0.08}$	$Mo_{0.50}V_{0.32}Te_{0.14}$	$Mo_{0.30}V_{0.23}Te_{0.06}$

TABLE 3: XPS Binding Energies (BE) of Mo−V−Te−O Catalysts Before and After Kinetic Studies

sample		Mo 3d5/2	V 3p3/2	Te 3d5/2	reported BE		
$Mo_{0.60}V_{0.30}Te_{0.10}$	before test	232.6	516.3	576.1	Mo 3d5/2	6+	232.8
	after	232.8	516.6	576.4		5+	232
$Mo_{0.50}V_{0.40}Te_{0.10}$	before Test	232.8	517.1	576.3	V 3p3/2	5+	517.6
	after	232.8	516.6	576.4		4+	516.3
$Mo_{0.30}V_{0.60}Te_{0.10}$	before test	232.6	516.6	576.1	Te 3d5/2	6+	576.6
	after	232.6	516.5	576.1		4+	575.7
TeO_2				575.5			
MoO_3		233.0					
V_2O_5			517.0				

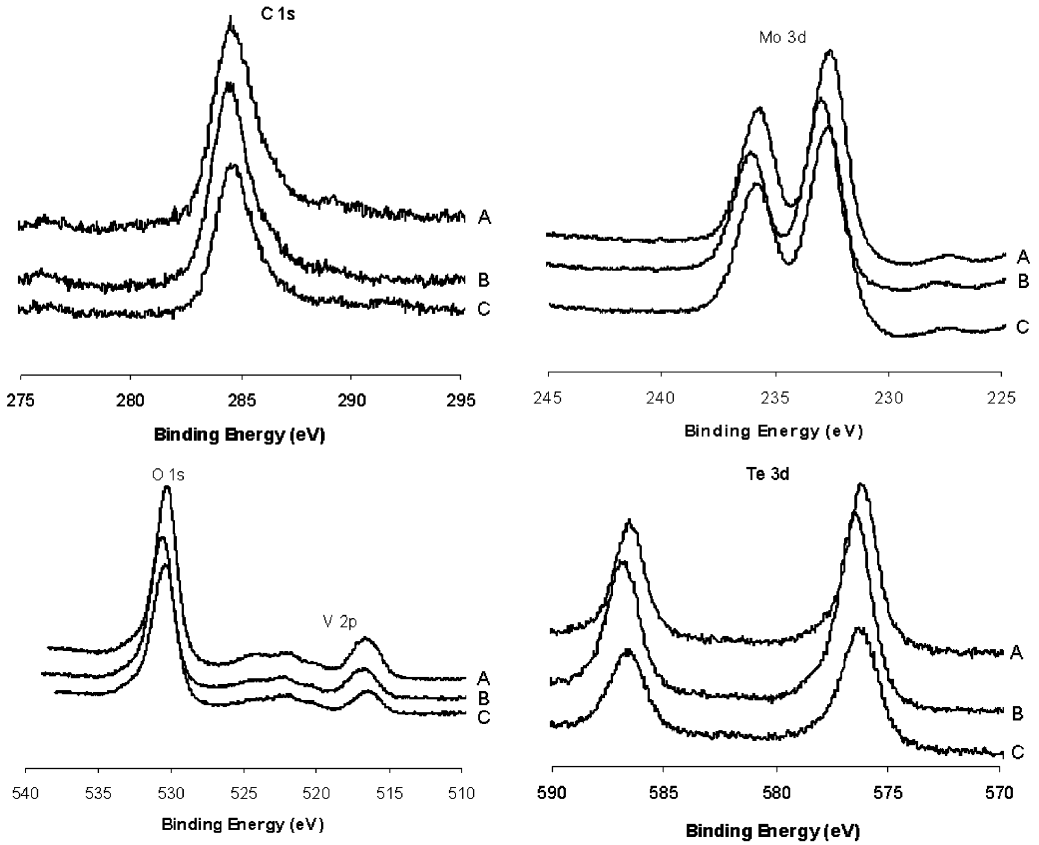

Figure 1. XPS spectra of Mo−V−Te−O catalysts after kinetic studies obtained at a 45° takeoff angle: (A) $Mo_{0.60}V_{0.30}Te_{0.10}$, (B) $Mo_{0.50}V_{0.40}Te_{0.10}$, and (C) $Mo_{0.30}V_{0.60}Te_{0.10}$.

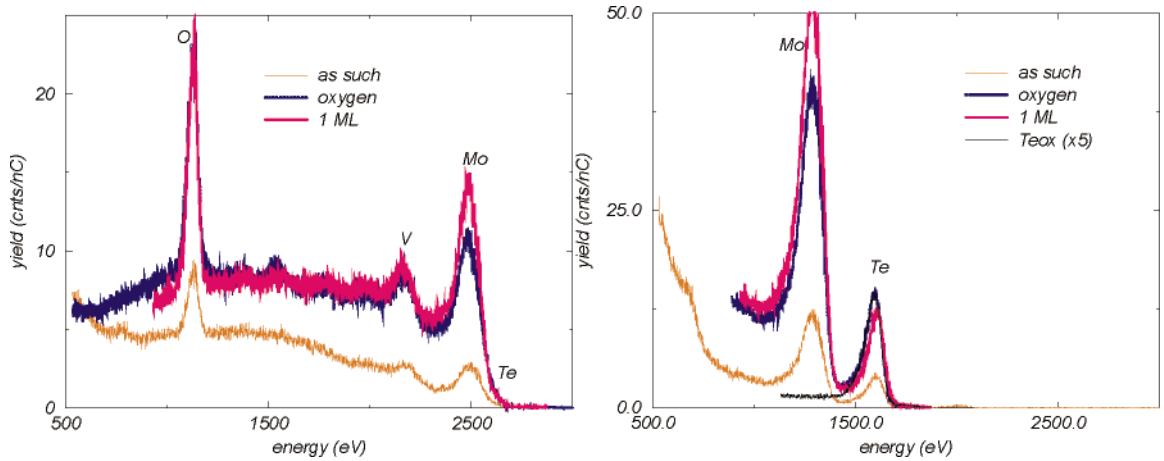

Figure 2. $^4He^+$ (left) and Ne^+ (right) LEIS spectra of the $Mo_{0.6}V_{0.3}Te_{0.1}$ catalyst.

The LEIS spectra of the three model catalysts ($Mo_{0.6}V_{0.3}Te_{0.1}$, $Mo_{0.5}V_{0.4}Te_{0.1}$, and $Mo_{0.3}V_{0.6}Te_{0.1}$) after kinetic studies are shown in Figures 2−4. The spectra on the left and right in Figures 2−4 correspond to the $^4He^+$ and Ne^+ spectra, respectively. Normalized LEIS signal yields were plotted in Figures 2−4 to enable a comparison of the LEIS spectra for these catalysts, i.e., the signal (in counts) per nanocoulomb (nC) of the incoming ion beam. The Ne^+ spectrum of the oxidized Te reference sample plotted at 20% scale of the original signal yield is also shown in Figures 2−4 for comparison. The LEIS spectra of the Mo−V−Te−O catalysts analyzed prior to atomic oxygen treatment showed the signals originating from the surface O, V, Mo, and Te atoms. The $^4He^+$ spectra showed combined Mo/Te peaks, whereas these peaks were clearly separated in the Ne^+ spectra. For the outermost surface of the $Mo_{0.5}V_{0.4}Te_{0.1}$ catalyst, a F signal corresponding to ∼10% of the monolayer coverage was detected as well. Most likely, the presence of this element was due to surface contamination with F of the Teflon liner used in synthesis.

After treatment with atomic oxygen, the O, V, Mo, and Te signals increased indicating that environmental contamination and/or carbonaceous product species were removed from the surface. The surface O signal after the atomic oxygen treatment did not result entirely from the original catalyst surface itself, but also from the atomic oxygen species adsorbed during this treatment. However, the relative intensities of the V, Mo, and Te signals did not appreciably change after the removal of surface contamination indicating that the surface reconstruction did not occur during the atomic oxygen treatment. The $Mo_{0.5}V_{0.4}Te_{0.1}$ catalyst underwent a second atomic oxygen treatment.

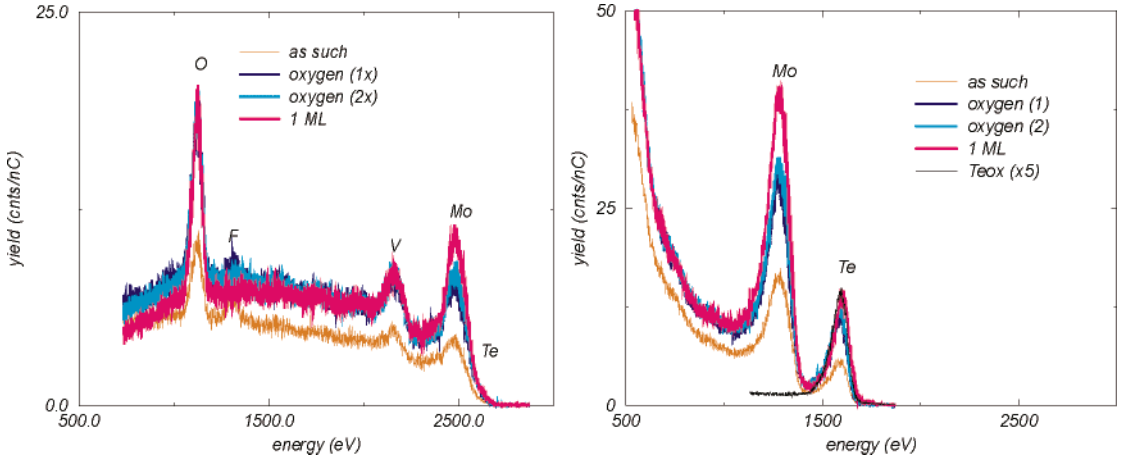

Figure 3. $^4He^+$ (left) and Ne^+ (right) LEIS spectra of the $Mo_{0.5}V_{0.4}Te_{0.1}$ catalyst.

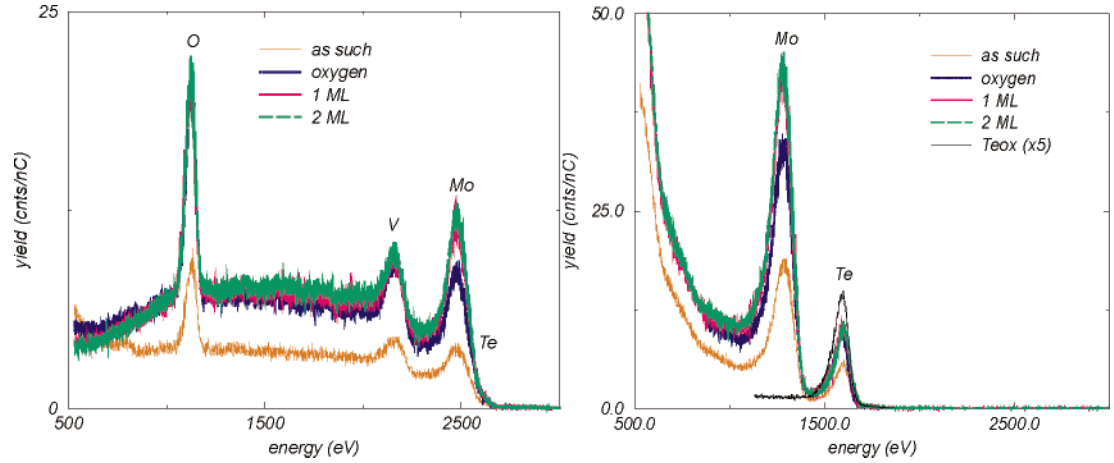

Figure 4. $^4He^+$ (left) and Ne^+ (right) LEIS spectra of the $Mo_{0.3}V_{0.6}Te_{0.1}$ catalyst.

TABLE 4: Surface Composition of Mo−V−Te Catalysts after Kinetic Studies

synthesis ratios	bulk	XPS composition (after KT)	LEIS (topmost)	LEIS (subsurface)
$Mo_{0.6}V_{0.3}Te_{0.1}$	$Mo_{0.60}V_{0.27}Te_{0.09}$	$Mo_{0.60}V_{0.25}Te_{0.08}$	$Mo_{0.60}V_{0.39}Te_{0.22}$	$Mo_{0.60}V_{0.25}Te_{0.15}$
$Mo_{0.5}V_{0.4}Te_{0.1}$	$Mo_{0.50}V_{0.30}Te_{0.05}$	$Mo_{0.50}V_{0.32}Te_{0.14}$	$Mo_{0.50}V_{0.51}Te_{0.21}$	$Mo_{0.5}V_{0.33}Te_{0.22}$
$Mo_{0.3}V_{0.6}Te_{0.1}$	$Mo_{0.30}V_{0.24}Te_{0.06}$	$Mo_{0.30}V_{0.23}Te_{0.06}$	$Mo_{0.30}V_{0.38}Te_{0.09}$	$Mo_{0.30}V_{0.25}Te_{0.08}$[a]

[a] Second subsurface (2 ML) composition: $Mo_{0.30}V_{0.22}Te_{0.05}$.

However, no significant changes in the intensities of the O, V, Mo, and Te signals were observed as a result of this additional treatment.

The LEIS peak areas were calculated by using a linear background subtraction procedure for all the samples and converted to the Mo−V−Te compositions (Table 4). The LEIS spectra reflecting the subsurface composition of these model catalysts were obtained after the removal of about one surface monolayer (1 ML) by Ne^+ sputtering. The ratio of LEIS signals obtained before and after sputtering of 1 ML scattered around 1.0 for O, V, and Te and 1.3 for Mo. These results indicated ~30% higher Mo content in the *subsurface* as compared to the topmost *surface*. Moreover, the surface Te content in the model Mo−V−Te−O catalysts was 1.5−4 times higher than that in the bulk (Table 4). Furthermore, the F signal was only present in the surface LEIS spectrum of the $Mo_{0.5}V_{0.4}Te_{0.1}$ catalyst. In the case of the $Mo_{0.3}V_{0.6}Te_{0.1}$ catalyst, a LEIS spectrum was also collected after the removal of a second monolayer, 2 ML (Figure 4), indicating a composition similar to that in the bulk (Table 4).

The effect of temperature on the topmost surface composition was further investigated for the $Mo_{0.5}V_{0.4}Te_{0.1}$ catalyst. This catalyst was heated at 5 °C/min to 400 °C inside the LEIS chamber and its LEIS spectra were collected after 10 min at 673 K (Figure 5). The LEIS spectra obtained showed a decrease for the F and V intensities and, to a minor extent, for Te. On the contrary, the Mo intensity increased slightly.

4. Discussion

Millet et al.[16,34] characterized the bulk mixed Mo−V−Te−Nb oxides containing a mixture of the M1 and M2 phases[37,45] by XPS. They found that the surface was depleted in V and enriched in Te, which was later confirmed for the M1 phase by Holmberg et al. on the basis of the XPS and ICP data.[15] The Mössbauer spectroscopy further showed that only Te^{4+} was present in the bulk, while Te^{6+} was detected at the surface by XPS.[34] Ueda et al.[46,47] investigated the catalytic functions of constituent metal oxides in propane oxidation to acrylic acid for three model orthorhombic (M1 phase) catalysts with bulk Mo−V−O, Mo−V−Te−O, and Mo−V−Te−Nb−O composi-

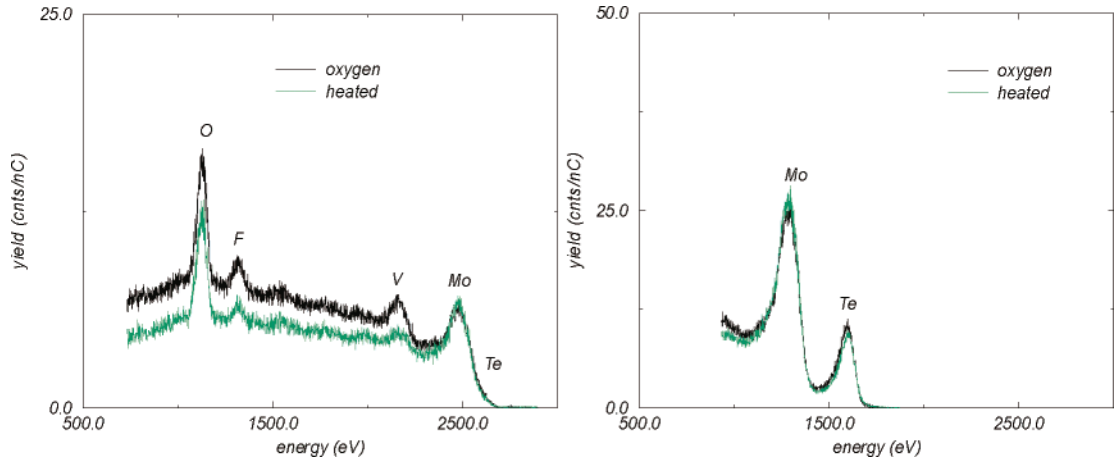

Figure 5. $^4He^+$ (left) and Ne^+ (right) LEIS spectra of the $Mo_{0.3}V_{0.6}Te_{0.1}$ catalyst before and after in situ heating at 400 °C for 10 min.

tions. All three catalysts showed very similar activity in propane oxidation; however, the Mo−V−O catalyst was unselective to acrylic acid. According to Ueda et al.,[47] the surface Te sites in these catalysts assisted propylene conversion to selective oxidation products, acrolein and acrylic acid. The presence of Nb on the surface isolated the active Mo and V sites and further increased the selectivity to acrylic acid by preventing its overoxidation over the Mo−V−Te−Nb−O catalysts. On the other hand, several recent studies established that the pseudohexagonal M2 phase was inefficient in propane (amm)oxidation.[14−16,28,38] However, some studies[14,16,38] indicated a synergy between the M1 and M2 phases during propane (amm)oxidation to acrylonitrile and acrylic acid over mixtures of these phases explained by the ability of the M2 phase to (amm)oxidize the propylene intermediate selectively.

DeSanto et al.[13,37] employed a combination of high-resolution TEM, synchrotron X-ray, and powder neutron diffraction methods and showed that V, Mo, and Te were present respectively in the 4+/5+, 5+/6+, and 4+ oxidation states in the M1 phase. They suggested that the M2 phase was inactive in propane oxidation because all vanadium in the bulk of the M2 phase was V^{4+} and proposed that in order to activate an alkane, V^{5+} must be neighbored by a less electronegative element such as Mo^{5+} or V^{4+}. Grasselli et al.[48] proposed that the active and selective surface has the structure of the bulk *ab* planes of the M1 phase (Figure 6) in which metal oxide octahedra (e.g. V^{5+}/Mo^{6+}) and Te^{4+}−O sites are stabilized and structurally isolated from one another by Nb^{5+} centers, each surrounded by the Mo−O octahedra. The V^{5+} surface sites through their resonance structure, $V^{5+}{=}O \leftrightarrow V^{4+}{\cdot}{-}O^{\bullet}$, are the alkane activating sites capable of methylene-H abstraction to form propylene. The Te^{4+} sites possessing a lone pair of electrons participate in the α-H abstraction from the formed propylene intermediate, while the adjacent Mo^{6+} sites are active and selective in the NH and O insertion into the π-allylic surface intermediate to form acrylonitrile and acrylic acid (from acrolein intermediate), respectively. A similar structural model of the active and selective surface was recently proposed by Solsona et al.[49] and Oliver et al.[50]

The M1 and M2 phases possessing well-defined rodlike crystal morphology were also obtained hydrothermally in the Nb-free system ($Mo_{0.6}V_{0.3}Te_{0.1}$) that showed moderate selectivity in transforming ethane and propane to ethylene and acrylic acid, respectively.[12,17,27,35] Previously reported model Mo−V−Te−O catalysts[30] contained predominantly (>95%) the M1 phase with the bulk Mo/V ∼2 ratio (Table 2). The bulk Mo/V ratios of the Mo−V−Te−O catalysts were close to the synthesis Mo/V

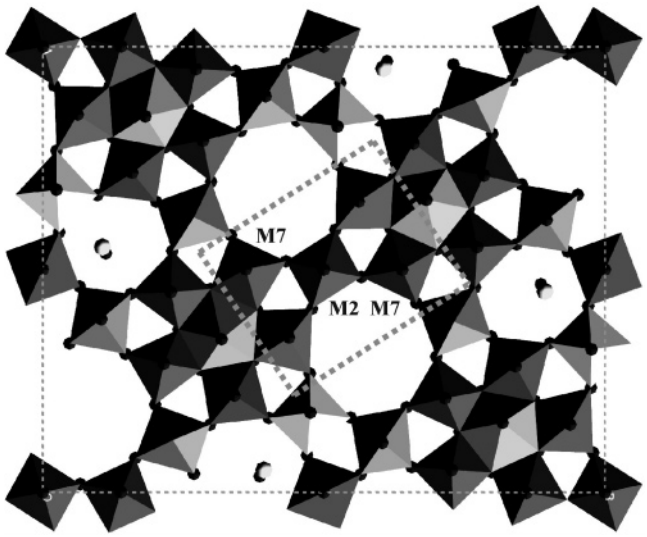

Figure 6. The *ab* planes of the M1 phase proposed to contain the M7−M2−M7 active and selective surface sites for propane (amm)oxidation.

compositions at the synthesis Mo/V ratios >1, while at the synthesis Mo/V ratio of 0.5 significantly less V was incorporated in the bulk of the $Mo_{0.3}V_{0.6}Te_{0.1}$ catalyst due to high Mo content of the orthorhombic M1 phase (Table 2). The $Mo_{0.5}V_{0.4}Te_{0.1}$ oxide being the pure M1 phase displayed the highest yield of acrylic acid (∼27 mol % at 380 °C and propane conversion of ∼65 mol %). The selectivity to acrylic acid over these model catalysts correlated with the extent of exposure of the surface *ab* planes of the M1 phase proposed to contain the active and selective surface sites.[12,14,27]

The XPS spectra collected at three different takeoff angles (Figure 1) were very similar for each Mo−V−Te−O catalyst probably due to random orientation of the catalyst particles. The surface-region compositions obtained by XPS were similar to the bulk (ICP) elemental compositions of all catalysts (Table 2). The similarity between the bulk and surface-region compositions may be explained by the fact that the latter are averaged over multiple subsurface layers, typically ∼1.5−6 nm below the topmost surface. Detailed information about the surface-region composition of these catalysts came from the LEIS studies, which are discussed in detail below. The XPS study of these catalysts before and after kinetic studies showed no significant changes in surface-region compositions with time on stream in agreement with previous observations.[35,51] These findings are also similar to those reported recently by Vitry et

al.[17] and Ueda et al.[47] for the $Mo_{0.6}V_{0.3}Te_{0.1}$ catalyst, which indicated only slight Mo enrichment in the surface region. On the contrary, in the case of Mo-rich hydrothermal Mo−V−Te−Nb−O catalysts (bulk Mo/V = 5), the XPS data indicated that the surface region was significantly enriched in Mo (Mo/V ∼9).[50]

The oxidation states of metal ions in the surface region were determined by comparing their XPS binding energies with the literature values for these metal ions in the various oxidation states.[44] The binding energies of Te^{4+} and Mo^{6+} ions in TeO_2 and MoO_3 references were similar to the published values.[44] Mo ions were found predominantly in the 6+ oxidation state, although some Mo^{4+} was also detected (Table 3). Vanadium was found as a mixture of the 5+/4+ oxidation states. Similar to earlier findings by Baca et al.,[16] the +4 and +6 oxidation states of Te were difficult to distinguish in the model Mo−V−Te−O catalysts, because the XPS binding energies of the Te^{4+} and Te^{6+} ions are very similar.[44] However, a Mössbauer and XPS study by Millet et al.[34] showed that the four-component $MoV_{0.33}Te_{0.22}Nb_{0.11}O_x$ catalyst prepared by the slurry evaporation method contained Te^{4+} in the bulk and mainly Te^{6+} in the surface region of the M1 and M2 phases in this catalyst.

The surface-region compositions of the model Mo−V−Te−O catalysts were obtained in the LEIS study. The comparison of the LEIS signals for O, V, Mo, and Te before and after atomic oxygen treatment indicated that the original catalysts had different surface concentrations of environmental contaminants and/or carbonaceous product species (Figures 2−4). The surface of the $Mo_{0.6}V_{0.3}Te_{0.1}$ catalyst had the highest coverage of these species (roughly 70%). There was no clear indication that any one of the elements (O, V, Mo, or Te) was preferentially covered by environmental contaminants and/or product species. It was concluded based on the LEIS signal yields observed for two subsequent oxygen treatments of the $Mo_{0.5}V_{0.4}Te_{0.1}$ catalyst (Figure 3) that less than 10% of the product species remained at the surface after the first atomic oxygen treatment.

The comparison of the topmost surface and bulk elemental compositions (Table 4) indicated that the outer surfaces of the model Mo−V−Te−O catalysts were enriched in V (∼1.4−1.7-fold excess) and Te species (∼1.5−4-fold excess) and thus depleted in Mo. The subsurface composition of all three catalysts determined after removing 1 ML by Ne^+ sputtering was similar to both their surface region (XPS) and bulk (ICP) compositions. It was further observed that the subsurface contained ∼30% more Mo than the topmost surface confirming that the outer surface of the Mo−V−Te−O catalysts was Mo-depleted. The signal of the F species disappeared from the LEIS spectrum of the $Mo_{0.5}V_{0.4}Te_{0.1}$ catalyst after the removal of 1 ML indicating that these species were a surface contaminant. The characteristic changes in the Mo, V, and Te concentrations as a function of distance from the topmost surface observed for the Mo−V−Te−O catalysts are plotted in Figure 7 for the $Mo_{0.3}V_{0.6}Te_{0.1}$ catalyst. The data shown in Figure 7 illustrated the differences in composition between the outer surface and the subsurface and bulk of the Mo−V−Te−O catalysts, while the subsurface and bulk compositions were similar. The LEIS data thus provided an explanation for the similarity between the surface-region compositions by XPS and the bulk compositions of the Mo−V−Te−O catalysts. Since only the topmost surface had notable differences in chemical composition from that of the bulk in the Mo−V−Te−O catalysts, the XPS technique essentially provided the bulk composition because it has the information depth of up to ∼10 atomic layers. Moreover, the LEIS findings suggested a structural model of an active and selective phase in which the bulk M1 phase is terminated by a *surface monolayer* highly efficient in propane transformation to oxygenates and acrylonitrile. No evidence of a *three-dimensional* nanophase (e.g. V_xO_y dispersed over the M1 phase and proposed as active and selective in propane (amm)-oxidation)[52,53] was obtained in the present LEIS study of the model Mo−V−Te−O catalysts.

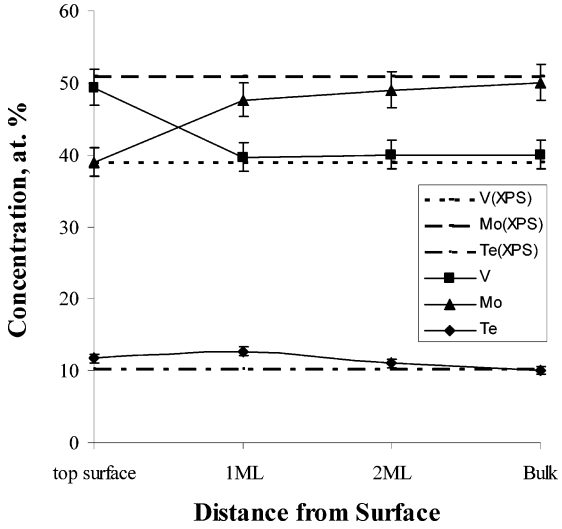

Figure 7. Mo, V, and Te concentration profiles in the surface region of the $Mo_{0.3}V_{0.6}Te_{0.1}O$ catalyst.

The effect of temperature (400 °C) representative of the typical fixed-bed conditions for propane (amm)oxidation on the topmost surface composition was investigated for one of the model catalysts ($Mo_{0.5}V_{0.4}Te_{0.1}$). The results obtained (Figure 5) showed that the V, F and, to a minor extent, Te signals decreased, while the Mo signal slightly increased at this high temperature. Apparently, fluorine was partially removed from the surface at high temperature together with vanadium as the more volatile V^{5+} fluoride species, which is characterized by the highest bond enthalpy (590 ± 63 kJ/mol) and vapor pressure (e.g., the boiling point of 48.3 °C for VF_5) among stable V and Mo fluorides.[54]

Since the bulk Mo−V−Te−O catalysts displayed certain structural characteristics of supported metal oxides, we compared their behavior in propane oxidation to that of supported Mo−V−O catalysts, in which MoO_x and VO_x were present as the surface species.[55] Bañares and Khatib [55] have recently investigated the molecular structures of alumina-supported Mo−V−O catalysts by Raman spectroscopy and characterized their catalytic activities in propane ODH. They observed that the surface Mo−V−O phases spread on the support as separate MoO_x and VO_x surface oxides at low surface coverage and formed various surface-supported three-dimensional Mo−V−O phases at above monolayer coverage depending on the ODH reaction conditions. They further observed that the supported Mo/V = 1 catalyst at the combined (Mo + V) monolayer coverage was the most active and selective in propane ODH to propylene among their supported Mo−V−O catalysts. Similar to their findings, the present kinetic study of propane oxidation to acrylic acid over the model bulk Mo−V−Te−O catalysts indicated that the most active and selective catalyst in this reaction, $Mo_{0.5}V_{0.4}Te_{0.1}$ (Table 1), possessed a Mo/V ratio of 1.0 in the topmost surface layer according to the LEIS data (Table 4). Furthermore, the selectivity to acrylic acid was a strong function of the topmost surface V concentration, while this trend was less significant for other reaction products (Figure 8). The optimal composition of the topmost surface layer in the model Mo−V−Te−O

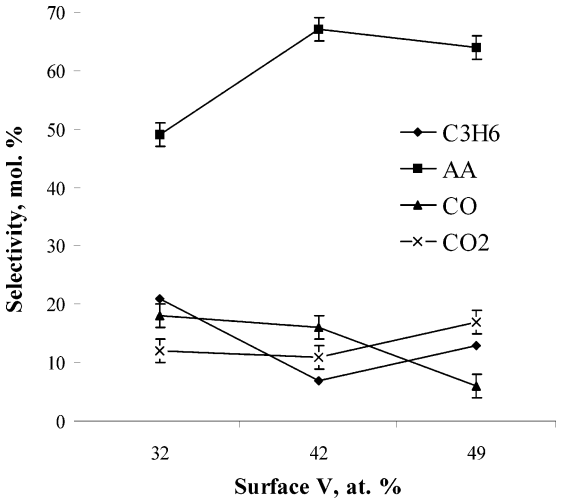

Figure 8. The selectivity to reaction products in propane oxidation over the Mo−V−Te−O catalysts as a function of V concentration in the topmost surface. Feed composition: 6.3 vol % of propane, 9.4 vol % of oxygen, 47.3 vol % of H_2O, and the balance He. Temperature: 380 °C. Propane conversion: 20−34%.

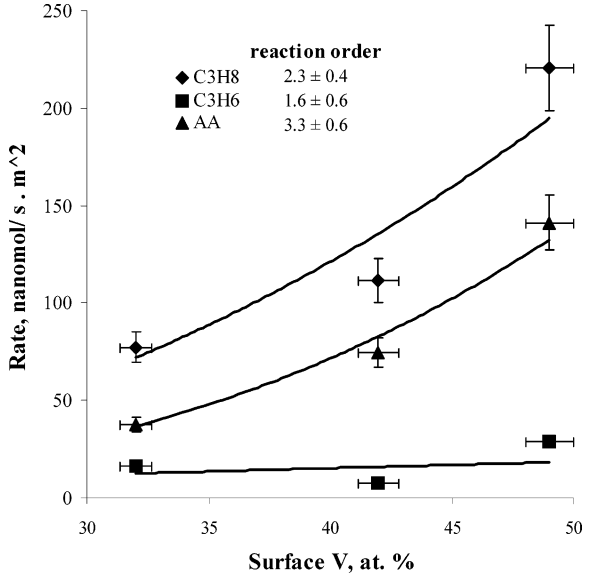

Figure 9. Intrinsic rates of propane consumption (C_3H_8) and formation of propylene (C_3H_6) and acrylic acid (AA) as a function of surface vanadium content at 380 °C and 20−34% propane conversion. Feed composition: 6.3 vol % of propane, 9.4 vol % of oxygen, 47.3 vol % of H_2O, and the balance He.

catalysts was close to $Mo_{0.50}V_{0.51}Te_{0.21}$ for the $Mo_{0.5}V_{0.4}Te_{0.1}$ catalyst (Figure 8), which displayed ∼27 mol % yield of acrylic acid at 49−68% propane conversion at 380−400 °C.[30]

Further insights into the nature of the active and selective surface sites of the model Mo−V−Te−O catalysts were obtained from correlations of the reaction rate data for the consumption of propane and formation of propylene and acrylic acid with the surface V concentration determined by LEIS (Figure 9). The reaction rate data shown in Figure 9 suggested that the rates of propane consumption and formation of propylene and acrylic acid correlated with the V concentration in the topmost surface layer. Moreover, no dependence of these reaction rates on either the surface Mo or Te concentrations was observed. These results suggested that the surface V oxide is the active and selective species not only in the initial step of propane activation and ODH to propylene, but probably also in subsequent steps of the allylic oxidation of propylene intermediate to acrolein and its oxidation to acrylic acid. The likely roles of the surface Mo and Te species in propane oxidation over the bulk Mo−V−Te−O catalysts are to tune the activity and selectivity of the surface V^{5+} oxide species by forming bridging V−O−M bonds and modify the surface acidity to control the residence times of the propylene and acrolein intermediates (and water) for the selective transformation of propane to acrylic acid.

Since V^{5+} was proposed as the propane-activating site,[14,48−50] we attempted to correlate the performance of the model Mo−V−Te−O catalysts with the surface vanadium content and probe whether a single or multiple surface vanadium sites were involved in propane activation. Previously, Smits et al.[56] employed LEIS to study the outermost surfaces of the mixed V−Nb−O catalysts for propane ODH to propylene. They reported an average reaction order of 2.0 ± 0.3 for propane consumption with respect to surface vanadium concentration determined by LEIS. They further observed that the intrinsic activity in propane ODH per surface vanadium site increased almost 4-fold as the surface V concentration increased from 10 to 50 mol %. Their findings further suggested that among possible types of surface active sites, i.e., single isolated VO_x sites, VO_x pairs, and larger VO_x ensembles, multiple VO_x sites were more active in propane ODH than the isolated sites. They proposed that surface VO_x ensembles were more active than isolated sites, because a bridging oxygen atom between two easily reducible vanadium ions was more active than an oxygen atom between a vanadium ion and a less easily reducible niobium ion in their V−Nb−O catalysts.

We adopted the method of Smits et al.[56] and plotted the rates of propane consumption and formation of propylene and acrylic acid with respect to the surface V concentration from LEIS, which are shown in Figure 9 for representative kinetic data at 380 °C. Average reaction orders of 2.3 ± 0.4, 1.6 ± 0.6, and 3.3 ± 0.6 were found to fit the data for respectively propane consumption and propylene and acrylic acid formation at 360−450 °C. It was difficult to determine accurately the dependence of these rates on the vanadium surface concentration given the error bars in Figure 9. However, these findings suggested that multiple surface VO_x sites are more efficient in propane activation and its oxidation to acrylic acid over Mo−V−Te−O catalysts than the isolated VO_x sites. An example of such a multiple surface VO_x site is a hypothetical surface M7−M2−M7 site proposed by Grasselli et al.[48] on the basis of the crystal structure of the bulk *ab* planes of the M1 phase (Figure 6). Such multiple VO_x sites are probably more efficient in propane oxidation to acrylic acid than the isolated VO_x sites, because they may provide four active O atoms required for this selective 8-e^- oxidation reaction. From a practical viewpoint, the results of this study strongly suggested further synthetic optimization of the topmost surface composition and the surface promotion of the M1 phase with metal oxide species to form new surface active V−O−M sites as two highly promising directions to enhance catalytic performance of these mixed metal oxides in propane oxidation to acrylic acid.

5. Conclusions

The Mo−V−Te−O catalysts possess relatively high activity and selectivity in propane oxidation to acrylic acid and represent well-defined model catalysts for elucidation of the surface molecular structure−activity/selectivity relationships.[30] The focus of this study was to obtain fundamental insights into the surface region composition of model Mo−V−Te catalysts by XPS and LEIS and the catalytic functions of V, Mo, and Te in these catalysts.

The LEIS study provided critical insights into the chemistries of outer surfaces and catalytic functions of V, Mo, and Te in propane oxidation over these multicomponent metal oxides. It demonstrated that the outer surfaces of the Mo−V−Te−O catalysts possessed somewhat different composition from those of the subsurface (XPS) and bulk (ICP), while the subsurface and bulk compositions were similar. These findings suggested a structural model of an active and selective phase in which the bulk M1 phase is terminated by a *surface monolayer* highly efficient in propane oxidation to acrylic acid. Among the Mo−V−Te−O catalysts studied, the optimal composition of the topmost surface layer for the selectivity to acrylic acid was close to $Mo_{0.50}V_{0.51}Te_{0.21}$ for the $Mo_{0.5}V_{0.4}Te_{0.1}$ catalyst, which displayed ∼27 mol % yield of acrylic acid at 49−68% propane conversion at 380−400 °C.[30]

The rates of propane consumption and formation of propylene and acrylic acid depended on the topmost surface V concentration, whereas no dependence of these reaction rates on either the surface Mo or Te concentrations was observed. Average reaction orders of 2.3 ± 0.4, 1.6 ± 0.6, and 3.3 ± 0.6 were found respectively for propane consumption and propylene and acrylic acid formation at 360−450 °C with respect to the topmost surface V concentration suggesting that multiple surface VO_x sites were more efficient in propane activation and formation of acrylic acid over the model Mo−V−Te−O catalysts than the isolated VO_x sites. These results suggested that the surface VO_x is the active and selective species not only in the initial step of propane activation and ODH to propylene, but also in the subsequent steps of the allylic oxidation of propylene intermediate to acrolein and acrylic acid. The results of this study have important practical consequences for the development of improved selective oxidation catalysts by introducing surface metal oxide components to form new surface active V−O−M sites for propane oxidation to acrylic acid.

Acknowledgment. This research was supported by the Chemical Sciences, Geosciences and Biosciences Division, Office of Basic Energy Sciences, Office of Science, U.S. Department of Energy under Grant No. DE-FG02-04ER15604. The LEIS study was conducted with financial support of the National Science Foundation (international supplement to NSF CAREER CTS-0238962 to V.V.G.) and Rohm and Haas Co.

References and Notes

(1) Thomas, J. M.; Thomas, W. J. *Principle and Practice of Heterogeneous Catalysis*; VCH Publications: New York, 1987.
(2) Satterfield, C. N. *Heterogeneous Catalysis in Practice*, 2nd ed.; McGraw-Hill: New York, 1991.
(3) Centi, G.; Cavani, F.; Trifirò, F. *Selective Oxidation by Heterogeneous Catalysis*: Kluwer Academic/Plenum Publishers: New York, 2001.
(4) Lin, M. *Appl. Catal., A* **2001**, *207*, 1.
(5) Grasselli, R. K. *Catal. Today* **1999**, *49*, 141.
(6) Bettahar, M. M.; Costentin, G.; Savary, L.; Lavalley, J. C. *Appl. Catal., A* **1996**, *145*, 1.
(7) Lin, M. *Appl. Catal., A* **2003**, *250*, 305.
(8) Lin, M. *Appl. Catal., A* **2003**, *250*, 287.
(9) Cavani, F.; Trifirò, F. *Catal. Today* **1999**, *51*, 561.
(10) Cavani, F.; Trifirò, F. *Stud. Surf. Sci. Catal.* **1997**, *110*, 19.
(11) Baerns, M.; Buyevskaya, O. *Catal. Today* **1998**, *45*, 13.
(12) Vitry, D.; Morikawa, Y.; Dubois, J. L.; Ueda, W. *Top. Catal.* **2003**, *23*, 47.
(13) DeSanto, P., Jr.; Buttrey, D. J.; Grasselli, R. K.; Lugmair, C. G.; Volpe, A. F.; Toby, B. H.; Vogt, T. *Top. Catal.* **2003**, *23*, 23.
(14) Grasselli, R. K.; Burrington, J. D.; Buttrey, D. J.; DeSanto, P., Jr.; Lugmair, C. G.; Volpe, A. F., Jr.; Weingand, T. *Top. Catal.* **2003**, *23*, 5.
(15) Holmberg, J.; Grasselli, R. K.; Andersson, A. *Top. Catal.* **2003**, *23*, 55.
(16) Baca, M.; Pigamo, A.; Dubois, J. L.; Millet, J. M. M. *Top. Catal.* **2003**, *23*, 39.
(17) Vitry, D.; Morikawa, Y.; Dubois, J. L.; Ueda, W. *Appl. Catal., A* **2003**, *251*, 411.
(18) *Kirk-Othmer Encyclopedia of Chemical Technology*, 4th ed.; Wiley: New York, 1991.
(19) Lin, M.; Linsen, M. W. U.S. Patent 6,180,825, 2001, to Rohm and Haas Company (USA).
(20) Takahashi, M.; Tu, X.; Hirose, T.; Ishii, M. U.S. Patent 5,994,580, 1999, to Toagosei Co., Ltd. (JP).
(21) Ushikubo, T.; Koyasu, Y.; Nakamura, H.; Wajiki, S. JP 10045664, 1998, to Mitsubishi Chemical Corp.
(22) Ushikubo, T.; Oshima, K. JP 10036311, 1998, to Mitsubishi Chemical Corp. (JP).
(23) Hatano, M.; Kayou, A. European Patent 318,295, 1988, to Mitsubishi Chemical Corp. (JP).
(24) Ushikubo, T.; Oshima, K.; Kayo, A.; Umezawa, T.; Kiyona, K.; Sawaki, I. European Patent 529,853, 1992, to Mitsubishi Chemical Corp. (JP).
(25) Katou, T.; Vitry, D.; Ueda, W. *Chem. Lett.* **2003**, *32*, 1028.
(26) Ueda, W.; Chen, N. F.; Oshihara, K. *Kinet. Catal.* **1999**, *40*, 401.
(27) Ueda, W.; Oshihara, K. *Appl. Catal., A* **2000**, *200*, 135.
(28) Botella, P.; López Nieto, J. M.; Solsona, B. *Catal. Lett.* **2002**, *78*, 383.
(29) Botella, P.; López Nieto, J. M.; Solsona, B. *Catal. Lett.* **2001**, *74*, 149.
(30) Guliants, V. V.; Bhandari, R.; Al-Saeedi, J. N.; Vasudevan, V. K.; Soman, R. S.; Guerrero-Pèrez, O.; Bañares, M. A. *Appl. Catal., A* **2004**, *274*, 123.
(31) López Nieto, J. M.; Botella, P.; Solona, B.; Oliver, J. M. *Catal. Today* **2003**, *81*, 87.
(32) López Nieto, J. M.; Botella, P.; Concepcion, P.; Dejoz, A.; Vazquez, M. I. *Catal. Today* **2004**, *241*, 91−92.
(33) Ushikubo, T.; Oshima, K.; Kayo, A.; Vaarkamp, M.; Hatano, M. *J. Catal.* **1997**, *169*, 394.
(34) Millet, J. M. M.; Roussel, H.; Pigamo, A.; Dubois, J. L.; Dumas, J. C. *Appl. Catal., A* **2002**, *232*, 77.
(35) Aouine, M.; Dubois, J. L.; Millet, J. M. M. *Chem. Commun.* **2001**, *13*, 1180.
(36) Botella, P.; Garcìa-González, E.; Dejoz, A.; López Nieto, J. M.; Vazquez, M. I.; González-Calbet, J. *J. Catal.* **2004**, *225*, 428.
(37) DeSanto, P., Jr.; Buttrey, D. J.; Grasselli, R. K.; Lugmair, C. G.; Volpe, A. F.; Toby, B. H.; Vogt, T. *Z. Kristallogr.* **2004**, *219*, 152.
(38) Holmberg, J.; Grasselli, R. K.; Andersson, A. *Appl. Catal., A* **2004**, *270*, 121.
(39) Al-Saeedi, J. N.; Vasudevan, V. K.; Guliants, V. V. *Catal. Commun.* **2003**, *4*, 537.
(40) Al-Saeedi, J. N. Ph.D. Dissertation, University of Cincinnati, 2003.
(41) Al-Saeedi, J. N.; Guliants, V. V.; Vasudevan, V. K. *Abstracts of Papers*; 225th National Meeting of the American Chemical Society, New Orleans, LA, March 23−27, 2003; American Chemical Society: Washington, DC, 2003.
(42) Maas, A. J. H.; Viitanen, M. M.; Brongersma, H. H. *Surf. Interface Anal.* **2000**, *30*, 3.
(43) Reijme, M. A.; van der Gon, A. W. D.; Draxler, M.; Gildenpfennig, A.; Janssen, F. J. J.; Brongersma, H. H. *Surf. Interface Anal.* **2004**, *36*, 1.
(44) *Handbook of X-Ray Photoelectron Spectroscopy*; Chastain, J., Ed.; Perkin-Elmer: Eden Prairie, MN, 1992.
(45) Garcìa-González, E.; López Nieto, J. M.; Botella, P.; González-Calbet, J. M. *Chem. Mater.* **2002**, *14*, 4416.
(46) Katou, T.; Vitry, D.; Ueda, W. *Catal. Today* **2004**, *237*, 91−92.
(47) Ueda, W.; Vitry, D.; Katou, T. *Catal. Today* **2004**, *96*, 235.
(48) Grasselli, R. K.; Buttrey, D. J.; DeSanto, P., Jr.; Burrington, J. D.; Lugmair, C. G.; Volpe, A. F., Jr.; Weingand, T. *Catal. Today* **2004**, *251*, 91−92.
(49) Solsona, B.; López Nieto, J. M.; Oliver, J. M.; Gumbau, J. P. *Catal. Today* **2004**, *91092*, 247.
(50) Oliver, J. M.; López Nieto, J. M.; Botella, P. *Catal. Today* **2004**, *96*, 241.
(51) Asakura, K.; Nakatani, K.; Kubota, T.; Iwasawa, Y. *J. Catal.* **2000**, *194*, 309.
(52) Schlögl, R.; Teschner, D.; Knop-Gericke, A.; Haevecker, M.; Kleimenov, E.; Su, D. *Abstracts of Papers*;228th National Meeting of the American Chemical Society, Philadelphia, PA, August 22−26, 2004; American Chemical Society: Washington, DC, 2004.
(53) Schlögl, R.; Hamid, A.; Niemeyer, D.; Timpe, O.; Idris, R. *Abstracts of Papers*, 228th National Meeting of the American Chemical Society, Philadelphia, PA, August 22−26, 2004; American Chemical Society: Washington, DC, 2004.
(54) Lide, D. R., Ed. In *Chemical Rubber Company Handbook of Chemistry and Physics*, 77th ed.; CRC Press: Boca Raton, FL, 1996.
(55) Bañares, M. A.; Khatib, S. J. *Catal. Today* **2004**, *96*, 251.
(56) Smits, R. H. H.; Seshan, K.; Ross, J. R. H.; van den Oetelaar, L. C. A.; Helwegen, J. H. J. M.; Anatharaman, M. R.; Brongersma, H. H. *J. Catal.* **1995**, *157*, 584.